Experimental evaluations on the shear behavior of fiber-reinforced calcareous sands

Houzhen Wei[1], Tao Zhao[2*], Qingshan Meng[1], Xinzhi Wang[1], Jianqiao He[3]

[1] State Key Laboratory Geomechanics and Geotechnical Engineering, Institute of Rock and Soil Mechanics, Chinese Academy of Sciences, Wuhan, 430071, China

[2] State Key Laboratory of Hydraulics and Mountain River Engineering, College of Water Resource and Hydropower, Sichuan University, Chengdu, 610065, China

[3] Guangxi Road and Bridge Engineering Group Co., Ltd, Nanning, 530011, China

* Corresponding author: Tel.: +86 28 8540 6701 E-mail: zhaotao@scu.edu.cn

Abstract: Fiber-reinforced calcareous sands manifest unique properties of increased shear strength and particle breakage. These features are of practical importance for some offshore engineering constructions because the strength improvement and efficient dense compaction of soils are both important. This paper presents the experimental evaluations on the characteristics of shear strength and particle breakage of fiber-reinforced calcareous sands by direct shear and ring shear tests with different vertical loading stress, fiber content and fiber length. In the tests, the mixture of fiber and sands can make the specimen a spatially interlocked and unitary coherent network, with efficient stress transmission. In addition, the overall deformation of sand specimen would increase with the fiber content due to low stiffness of fiber elements. Thus, in direct shear tests, the secant elastic modulus decreased, while the shear strength increased with the fiber content. The contribution of fiber elements to the shear strength of sand specimen came mainly from the friction and tension forces exerted when they were deformed. These two types of force could mobilize the additional shear resistance of sands, and thus increase the overall shear strength of the sample. In ring shear tests, the breakage intensity of calcareous sands increased with the vertical loading stress, fiber content and fiber length. At low fiber content and length, the inter-particle contacts and interlocking effects influenced the shear strength and particle breakage significantly, while at higher fiber content, the role of fiber friction and tension forces became dominant.

Keywords: fiber reinforcement, calcareous sands, direct shear test, ring shear test, shear band, particle breakage

Introduction

Randomly distributed short fiber elements have been widely used for soil reinforcement due to their tension-resisting properties to improve soil strength with simple engineering practices (Maher and Gray, 1990, Yetimoglu and Salbas, 2003). The inclusion of fibers into soils can to some extent mimics the plant roots which improves the strength and stability of soil (Diambra et al., 2010). In some engineering projects, the fiber-reinforced soils can be used to stabilize slopes, strengthen foundations and footings. As stated by Maher and Gray (1990), the fibers can effectively interlock soil particles as a spatially three-dimensional unitary and coherent matrix and thus restrict their displacements. When relative shear displacement occurs within the compacted soil sample, the sand particles would compress and abrade the fiber surface, leading to plastic tensile deformation of the fiber elements. The tensile force would in turn act on the sand particles, resisting their shear deformations (e.g. particle rearrangements). The reinforcement efficiency of fiber depends on the particle size / shape, gradation and soil dry density, as well as the fiber properties (e.g. strength, modulus, roughness, length and content) (Santoni et al., 2001, Yetimoglu and Salbas, 2003). To guarantee good performance, the fiber elements should also be long and frictional enough to prevent pull-out under shear deformations (Maher and Gray, 1990).

As stated in Tang et al. (2016), the interfacial interactions between fiber surface and soil particles would contribute to the shear strength of fiber-reinforced soil, which depends heavily on the soil compaction and shear deformation. Fibers with high surface roughness can lead to efficient mechanical interlocking and load transferring between sand particles. This effect of strength reinforcement becomes increasingly evident for soils with high dry density and fiber content (Consoli et al., 2011). Yetimoglu and Salbas (2003) investigated the shear strength of fiber-reinforced sands by direct shear tests. They concluded that the fiber content has a negligible influence on the peak strength and initial stiffness of sands. However, the fiber reinforcement can effectively reduce the soil brittleness, such that the loss of post-peak shear strength can also be reduced effectively, or equivalently the increase of residual strength (Consoli et al., 2009, Salah et al., 2010). Diambra et al. (2010) tested the mechanical behaviour of fiber-reinforced quartzitic sands by triaxial compression and extension experiments. They stated that the sample preparation procedure will inevitably make the fiber elements distribute along sub-horizontal orientations, such that the potential weak layers or localized deformation planes will preferably occur along that direction. By performing ring shear experiments on glass beads, Jiang et al. (2017) observed that the shear stress has apparent periodic fluctuations, which reflects the gradual building up and subsequent releasing of shear resistance. In this process, the particle friction and interlocking can contribute significantly to the granular shear strength. When particle slippage or breakage occurs, the shear resistance would drop suddenly, which is accompanied by acoustic energy emissions. Fatahi et al. (2012) discussed the mechanical responses of soft clays treated with cement and different types of fiber. They concluded that fiber reinforcement can increase the compressive strength and make the brittle cemented soil more ductile. The use of carpet and steel fibers can effectively increase the tensile strength, while almost no influence was found for polypropylene fibers (Fatahi et al., 2013). In these tests, the characteristics of cementation bond breakage and fiber rupture can be analysed effectively by a non-linear constitutive model, as reported in Nguyen and Fatahi (2016).

In addition, the inclusion of fibers into soil can also influence the hydraulic properties of soil significantly. Ibraim et al. (2010) found that the fiber reinforcement inclusions in quartzitic sands can effectively reduce the potential of soil liquefaction under monotonic loading and the reinforced soil manifests a strain hardening response. The effective stress paths for tests with different fiber contents would finally reach a common path. By performing the undrained ring-shear tests on saturated fiber-reinforced sands, Liu et al. (2011) observed that the fiber reinforcement has a great influence on the undrained shear behaviour of medium dense and dense silica sand samples with a clear increase of shear strength, but no significant influence on loose samples. In particular, the fiber-reinforcement can effectively prevent soil liquefaction and the shear resistance fluctuates even after the shear failure has happened. This effect becomes increasingly evident for samples with high fiber contents. Estabragh et al. (2014) observed that the fiber reinforcement can effectively reduce the fluid seepage velocity in silty sands, and thus increase its piping resistance. This effect is closely related to the fiber content and length.

Most previous studies have investigated the mechanical response of quartzitic sands / clay reinforced by randomly distributed fibers, while little attention has been given to the highly porous and brittle calcareous sands. The unique features of fiber-reinforced calcareous sands are the increase of shear strength and particle breakages under relatively low external loading stresses. In fact, the breakage of calcareous sands has been widely observed in offshore engineering projects under certain stress and strain conditions (Coop et al., 2004, Wu et al., 2014, Yu, 2017), which would sometimes cause serious problems during pile driving (Wang et al., 2011). According to Oldecop and Alonso (2007), the crushed sands can be packed efficiently under normal consolidating stresses by filling the pre-existing voids with fine sand fragments, resulting in densification and settlement of the soil. This feature has a significant influence on the mechanical response of reinforced calcareous sands, such as the shear resistance and deformation (Hardin, 1985). As an increasing number of offshore engineering constructions involve calcareous sands, it is necessary to investigate the mechanical response and particle breakage characteristics of calcareous sands when fiber reinforcement is used. In particular, experiments are needed to clarify the potential enhancements of soil shear strength and particle breakage intensity for the fiber-reinforced soil specimen at large shear deformations, as presented herein. This paper is organized as follows: firstly, the experimental configurations are given. Then, the results of the direct shear and ring shear tests are presented, with respect to the characteristics of shear stress and particle breakage. Thirdly, a detailed discussion of particle breakages for different experimental conditions are given. The final section gives out a summary of major conclusions reached in this study.

Experimental Configurations

The experimental investigations include a series of consolidated and drained (CD) direct shear and ring shear tests, aiming to investigate the shear strength and particle breakage characteristics of fiber-reinforced calcareous sands. These testing conditions were employed to consider the pile driving process in highly permeable calcareous soils at relatively low shear speeds. The sand specimens were sampled from Yongshu Coral Reef, South China Sea (Wang et al., 2011). The chemical composition of the calcareous sands consists of mainly aragonite (CaCO3, ≈ 68%) and magnesian calcite ((Ca, Mg)CO3, ≈ 32%). The properties of calcareous sands and polypropylene fibers are listed in Table 1. In this study, we used a relatively coarse and uniformly graded calcareous sands of diameter [1, 2] mm, which were mixed with short polypropylene fibers of various contents and lengths. The calcareous sands were chosen for a better illustration of particle breakages during the ring shear tests, because the coarse and uniformly graded sands can be crushed readily under relatively low vertical loading stress (Bolton et al., 2008). The fiber content (w_f) in the reinforced sand specimen is defined as the generally used one:

$$w_f = m_f / m_s \tag{1}$$

where m_f is the mass of polypropylene fibers and m_s is the mass of dry calcareous sands. In a series of sensitivity studies, w_f was set as 0%, 0.25%, 0.5%, 0.75% and 1%, respectively. A plan view photo of the mixture sample of various fiber contents is shown in Fig. 1.

In the direct shear tests, the sample was cylindrical with the radius of 61.8 mm and height of 20 mm, while in the ring shear tests, the sample had dimensions of 150 mm of outer diameter (OD), 100 mm of inner diameter (ID) and 20 mm of height. The ring shear (RS) testing apparatus used in this study consists of three major parts: ring shear box, loading control system and data acquisition system as shown in Fig. 2. The sample preparation and testing procedures were set the same as those detailed in Wei et al. (2018). A brief introduction of the procedures employed for void ratio determination and sample preparation according to the Chinese Standard of Soil Test Method is given as below.

The maximum void ratio:

1) A fixed mass of 700g dry sands (m_d) are poured slowly into a 1000 ml glass measuring cylinder (inner diameter ≥ 6 cm).
2) The upper surface of the sands is scraped gently to flat. Then, the bulk sand volume can be measured.
3) Repeat the procesures 1) and 2) for several times and record the maximum sand volume (V_{max}).
4) The minimum dry sand density (ρ_{dmin}) is calculated as $\rho_{d\min} = m_d / V_{\max}$. The maximum void ratio is calculate as $e_{\max} = \rho_w G_s / \rho_{d\min} - 1$, with G_s being the specific gravity of sand particles. In this study, e_{max} of the loose calcareous sand sample is measured as 1.657.

The minimum void ratio:

1) A specific mass (m_0 = 600~800g) of dry sands are slowly poured into a cylindrical metal container (inner diamter = 10 cm, height = 12.75 cm).

2) Hit the upper surface of the sands by a driving hammer (1.25 kg; diameter = 5 cm; falling height = 15 cm) for 30~60 times per minute until the sand volume remain constant.

3) Pour the second and third layer of sands into the container (with the same specific mass (m_0) in each layer), following the same consolidation procedure in 2).

4) Measure the final stable volume of the sample as V_{min} and dry sand mass as m_d.

5) The maxmum dry sand density (ρ_{dmax}) is calculated as $\rho_{d\max} = m_d / V_{\min}$. The minimum void ratio is calculate as $e_{\min} = \rho_w G_s / \rho_{d\max} - 1$. In this study, the e_{min} of the dense calcareous sand sample is measured as 1.385.

Sample preparation:

1) Based on the relative density $\left(D_r = \dfrac{e_{\max} - e_0}{e_{\max} - e_{\min}} = \dfrac{(\rho_d - \rho_{d\min})\rho_{d\max}}{(\rho_{d\max} - \rho_{d\min})\rho_d} \right)$ of sand sample (D_r = 1.05~1.17, measured for sand samples used in this study) and the sample volume, the aimed dry sand mass (m_d) can be calculated.

2) Mix the sands with short polypropylene fibers uniformly. Then, the mixed sample is carefully poured into the container of testing apparaturs (direct shear box or ring shear box). In this process, a smooth glass rod (6 mm in diameter) is used to tap the upper surface of the sand specimen gently so that the aimed height can be reached.

3) Distilled water is poured slowly onto the upper surface of the sand specimen, until a fully saturated state is reached. Then, the loading and shearing systems are installed in place. The aimed vertical loading stress is applied on the sample until it is fully consolidated. Normally, this process will take 24 hours.

4) The consolidated specimen will be used for direct shear or ring shear tests. The maximum shear displacement for the direct shear and ring shear tests are 8.8 mm and 16000 mm, respectively.

In preparing the sample, there is a limit mass content of fibers mixed in the calcareous sands, so that below this value, the fiber-sand mixtures can be prepared uniformly (e.g. avoid any sand segregation). This limit value is closely related to the relative density (or target void ratio) of the mixture and it may vary widely for different types of sands. According to Diambra et al. (2010), a fiber mass content of 1% can be reached at the maximum void ratio (e = 1). The mixture of fibers in sands would increase the tendency of particle segregation, which becomes increasingly evident for samples with high fiber contents. Thus, the maximum value of w_f is set as 1% in the current study. In addition, the random and uniform distribution of discrete fiber elements within the sands can also maintain the isotropy of soil strength (Yetimoglu and Salbas, 2003). Thus, in this study, the sand-fiber mixtures were poured slowly into the testing box in two layers, tamping after each layer to obtain a uniform distribution of fibers within the sands. A set of fiber lengths, i.e. 3 mm, 6 mm, 9 mm and 12 mm, were used in a series of sensitivity studies.

Results

Direct shear tests

The direct shear tests were employed in this study to evaluate the stress-displacement response of fiber-reinforced calcareous sands. Fig. 3 (a) presents the shear stress-displacement relationship of the fiber-calcareous sands mixture under different vertical loading stresses. It can be seen that the initial tangential stiffness of the fiber-reinforced sands was the same for each test, while the final stable value of shear strength increased with the vertical loading stress. According to the shear strength data plotted on Fig. 3 (b), it is straightforward to calculate the typical shear strength parameters, namely the internal friction angle (φ) of 33.2° and the cohesion (c) of 170 kPa. It should be noted that the calculated soil cohesion is not a representation of actual internal cohesive forces between particles, but the interlocking effects of highly angular calcareous sands and intertwined fiber distributions. For direct shear tests on samples with various fiber contents (see Fig. 4), the initial sample stiffness and final stable shear stress were the same, while the shear stress at small shear displacement (≤ 6 mm) decreased with the increasing fiber content. The independence of initial stiffness on fiber content can match well the observations in Karla Salvagni et al. (2005). This result is as expected because at relatively small shear displacement, the contributions of shear resistance came mainly from the inter-particle friction and interlocking in the vicinity of the points where a sand particle was in contact with adjacent particles, while the fiber friction and tension were not well exerted (see the inset plot (a)). Since the number of solid contacts is inversely proportional to the fiber content, the shear strength would decrease with the fiber content at relatively small shear deformations. In general, the exertion of fiber strength requires a large relative displacement between the fiber element and sand particles (see the inset plot (b)). Thus, at large shear displacement (> 6 mm), the shear strength of the fiber-sand mixture with high fiber content increased faster than that of tests with low fiber content. Due to the relatively short shear displacement occurred in the current direct shear tests, the final stable shear stress for all the tests can only reach approximately the same value at a shear displacement of 8 mm. However, the general increasing trend of shear stress with fiber content indicates that the final stable shear strength of fiber-reinforced sands would increase with the fiber content if the sample can deform to a larger displacement.

Fig. 5 illustrates that the shear strength of the fiber-calcareous sands mixture increases with the fiber length. In the test, the shear strength of the sample came mainly from the friction and interlocking between sand particles, the friction and tension forces of fiber elements. The longer fiber elements can interact with more sand particles by abrasions than the shorter ones. As a result, the force transmission within the sample can be more effective and the solid materials can deform more coherently as a whole during shear deformations. The contribution of fibers to the shear strength of soil resulted mainly from the fiber distortion (e.g. stretching, slipping, or breaking) during sample deformations (Maher and Gray, 1990). In this process, the tensile force in fiber can be divided into the tangential and normal components acting on sands in the shear zone. The normal force component can increase the confining stresses acting on the shear zone, and thus mobilized the additional shear resistance. Meanwhile, the tangential force component can directly resist shear displacement. During the tests, partial slippages of fibers may occur because the fibers and sand particles were interacted with each other only by friction. Thus, stress fluctuations can be observed in the stress-displacement curves, particularly for tests with short and high content fibers (see Fig. 4 and Fig. 5).

Ring shear tests

The ring shear tests were employed in this study to analyze the particle breakage characteristics of the fiber-reinforced calcareous sands. This approach allows the sand particles to break thoroughly at large shear deformations (Coop et al., 2004), mimicking the natural and engineering shearing processes, such as slope failure and pile driving. The intensity of particle breakage can be quantified by analyzing the particle size distribution (PSD) of the sample after the ring shear tests. As stated by Zhang et al. (2015), the PSD is a unique characteristic parameter of a soil specimen, determining its physical and mechanical properties (e.g. particle size and shape, stress-strain behavior). In soil constitutive modeling, the inclusion of PSD as a variable is necessary for considering particle breakages and variations of mechanical behavior (Einav, 2007, Muir Wood and Maeda, 2007, Yu, 2017). Thus, the PSD curve can be a good indication of particle breakage intensity by comparing the percentage of crushed grains finer than the initial particle size grading. In this study, the calcareous sands in the shear band were carefully retrieved from the shear box after each test. Then, the PSDs of coarse grains were analyzed via wet-sieving by hand, while fine particles smaller than 0.074 mm were analyzed by the laser diffraction particle size analyzer.

Fig. 6 illustrates the PSD curves of calcareous sands after the ring shear tests under various vertical loading stresses. According to the figure, it can be seen that particle breakage occurred during each test and its intensity increased with the vertical loading stress. During the test, the high vertical loading stress would consolidate the fiber-sand sample to a dense state with frequent particle contacts and effective interlocking. This dense state of particle packing would also facilitate the force transmission and subsequent particle breakages under shear deformations. Thus, the shearing process can produce a large amount of fine grains with sizes smaller than 0.1 mm.

For tests with different fiber contents, the obtained PSD curves are shown in Fig. 7. In the figure, the difference between the PSD curves of each test is very small. However, the general trend is that the percentage of fine grains increased with the fiber content, except for w_f =0%. This result is as expected because the existence of fibers within the calcareous sand sample can transfer particle interaction forces via abrasion and tension. In addition, the particle interlocking can also act more effectively as particles were packed closely under the fiber tension forces. Thus, the combined force contributions from fiber tension and particle interlocking would increase the shear resistance of the sand-fiber mixture. This effect was particularly significant for tests with high fiber contents. However, it is worth noting that the fiber friction and tension forces are only active at relatively large shear deformations. For tests on pure calcareous sands (w_f=0%), the PSD curve after the ring shear test just lies in the middle of other curves because the particle friction and interlocking also contributed significantly to sand particle breakages. This result indicates that the addition of fibers into the sand sample can to some extent curtail the breakage of sand particles, such that the pure sand sample experienced higher breakage than the fiber-reinforced sands. According to Santos et al. (2010) and Miranda Pino and Baudet (2015), this is because the energy lost in deforming and breakage of fiber elements would reduce the energy for crushing particles. However, in Fig. 7, a threshold value of fiber content (w_f = 0.5%) seems to exist, above which the addition of fibers can still lead to higher sand breakages than the pure sand sample.

The detailed information of crushed particles in the shear band, such as the surface characteristics and particle arrangements, can be obtained by the Scanning Electron Microscopy (SEM) images, as shown in Fig. 8. For comparison purpose, the SEM image of a single calcareous sand particle is also presented in Fig. 8 (f). According to the figure, the intact calcareous sand had an angular shape, with very rough surface and well-developed small voids. The porous structure was also fundamental for the calcareous sands to be crushed readily into very fine grains under external loadings. At low fiber content ($w_f \leq$ 0.25%, Fig. 8 (a) and (b)), the surface of sand specimen was generally rough, and several coarse grains, cracks and large void space can be clearly identified. However, for tests of higher fiber contents ($\geq$ 0.5%), the cracks and void space in the surface of sand specimen decreased gradually with the fiber content, as more fine sands existed to fill up these spaces (see Fig. 8 (c), (d) and (e)). This phenomenon is as expected because the increase of fiber content can lead to a more complete particle breakages in the shear band, producing a large number of fines (< 0.074 mm). These fine sands could fill up the void spaces effectively, creating a densely packed specimen. Meanwhile, the existence of fibers within the specimen would inevitably create a relative rough surface when sampling the sands from the shear band, as shown in Fig. 8 (d) and (e).

Fig. 9 shows the PSD curves of ring shear tests on calcareous sands reinforced by fibers with various lengths. According to the plot, it can be observed that the intensity of particle breakage increased with the fiber length, indicating that long fibers were more efficient in increasing the shear stresses within the soil sample. The influence of fiber length on particle breakage characteristics was very limited for short polypropylene (< 10 mm), such that the PSD curves were almost identical to that of pure sand specimen.

Discussion

The ring shear tests presented in this study were aimed at investigating the shear behavior (e.g. mechanical behavior and breakage characteristics) of fiber-reinforced calcareous sands at relatively large shear deformations. It is apparent that the extent of particle breakage can vary significantly for different testing conditions, such as vertical loading stress, fiber content and fiber length. Thus, it is necessary to employ a unique parameter to quantify the particle breakage intensity and relate it to specific testing conditions employed in this study. Here, the widely accepted relative breakage (B_r) by Hardin (1985) has been adopted in the analyses due to its advantage of representing particle grading changes as a single simple parameter. The definition of B_r is illustrated in Fig. 10 (d), as the ratio of total particle breakage (area B) to the potential breakage (sum of area A and B) (see also Yu (2017) and Bowman et al. (2012)). According to the PSD curve of each test (see Fig. 6, Fig. 7 and Fig. 9), the relative particle breakage of fiber-reinforced sands can be summarized as a function of the vertical loading stress (σ), the fiber content (w_f) and the fiber length (l), as shown in Eq. (2).

$$B_r = f\left(\sigma,\ w_f,\ l\right) \tag{2}$$

Fig. 10 (a) shows that the relative breakage of calcareous sands increased linearly with the vertical loading stress (σ). For different tests, the increase of σ would compress the fiber-sand mixture to a dense state, increasing the inter-particle stresses. As a result, the ring shearing process can easily crush these closely packed and interlocked particles, increasing the value of B_r. Fig. 10 (b) illustrates that the relative breakage of calcareous sands increased with the fiber content, following approximately an exponential relationship. Under the current testing configuration, the particle breakage intensity remained relatively small at low fiber content ($w_f \leq 0.5\%$), while it increased quickly to a large value at higher fiber contents. This result indicates that the friction and interlocking effects between sand particles were dominant for particle breakages in tests of low fiber contents, while the fiber friction and tension were dominant in tests of high fiber contents. Fig. 10 (c) presents a correlation relationship between B_r and fiber length (l). It can be seen that except for the case of l = 9 mm, B_r increased linearly with l. The increasing pattern of B_r is as expected because long fibers were more effective at transferring friction and tension forces to the surrounding calcareous sands, resulting in particle breakages in a relatively large area. However, the relatively low value of B_r for l = 9 mm may result from the scattering error of sample preparation in analyzing particle size distribution (see also Fig. 9).

Conclusions

This paper presents experimental results of a series of direct shear and ring shear tests on fiber-reinforced calcareous sands of various initial conditions, e.g. loading stress level, fiber content and fiber length, aiming to investigate the characteristics of stress-displacement evolution and particle breakages. In the tests, the short polypropylene fibers have been proved effective in reinforcing the calcareous sands, regarding the increases of shear strength and particle breakage intensity. The main conclusions can be summarized as follows:

1) The distribution of fibers in calcareous sands made the specimen a spatially interlocked and unitary coherent granular assembly, with effective contact force transmissions during the shearing tests. The contribution of fibers in improving the shear strength of calcareous sands came mainly from the friction and tension forces exerted by fiber elements when external loads were applied. These froces can effectivley increase the local confining stress on the shear zone and thus resist shear deformations.

2) The shear strength and particle breakage intensity of calcaresous sands increased with the vertical loading stress, fiber content and fiber length. At low fiber content and fiber length, the inter-particle friction and interlocking effects were dominant during shear deformations, while at higher values, the fiber friction and tension forces had a significant influence on the strength and particle breakge characteristics of the fiber-reinforced calcareous sands.

Acknowledgements

This research was supported by the Strategic Priority Research Program of Chinese Academy of Sciences (grant XDA19060301), National Natural Science Foundation of China (grant 41372316, 41572297 and 41602289), Youth Innovation Promotion Association of CAS (grant 2015272). All these supports are acknowledged.

References

Bolton, M. D., Nakata, Y., and Cheng, Y. P. (2008). "Micro- and macro-mechanical behaviour of DEM crushable materials." *Géotechnique,* 58(6), 471-480.

Bowman, E. T., Take, W. A., Rait, K. L., and Hann, C. (2012). "Physical models of rock avalanche spreading behaviour with dynamic fragmentation." *Canadian Geotechnical Journal*, 49(4), 460-476.

Consoli, N. C., Casagrande, M. D. T., Thomé, A., Rosa, F. D., and Fahey, M. (2009). "Effect of relative density on plate loading tests on fibre-reinforced sand." *Géotechnique*, 59(5), 471-476.

Consoli, N. C., Moraes, R. R. d., and Festugato, L. (2011). "Split tensile strength of monofilament polypropylene fiber-reinforced cemented sandy soils." *Geosynthetics International*, 18(2), 57-62.

Coop, M. R., Sorensen, K. K., Freitas, T. B., and Georgoutsos, G. (2004). "Particle breakage during shearing of a carbonate sand." *Géotechnique*, 54(3), 157-163.

Diambra, A., Ibraim, E., Muir Wood, D., and Russell, A. R. (2010). "Fibre reinforced sands: Experiments and modelling." *Geotextiles and Geomembranes*, 28(3), 238-250.

Einav, I. (2007). "Breakage mechanics—Part I: Theory." *Journal of the Mechanics and Physics of Solids*, 55(6), 1274-1297.

Estabragh, A. R., Soltannajad, K., and Javadi, A. A. (2014). "Improving piping resistance using randomly distributed fibers." *Geotextiles and Geomembranes*, 42(1), 15-24.

Fatahi, B., Fatahi, B., Le, T. M., and Khabbaz, H. (2013). "Small-strain properties of soft clay treated with fibre and cement." *Geosynthetics International*, 20(4), 286-300.

Fatahi, B., Khabbaz, H., and Fatahi, B. (2012). "Mechanical characteristics of soft clay treated with fibre and cement." *Geosynthetics International*, 19(3), 252-262.

Hardin, B. O. (1985). "Crushing of Soil Particles." *Journal of Geotechnical Engineering*, 111(10), 1177-1192.

Ibraim, E., Diambra, A., Muir Wood, D., and Russell, A. R. (2010). "Static liquefaction of fibre reinforced sand under monotonic loading." *Geotextiles and Geomembranes*, 28(4), 374-385.

Jiang, Y., Wang, G., and Kamai, T. (2017). "Acoustic emission signature of mechanical failure: Insights from ring-shear friction experiments on granular materials." *Geophysical Research Letters*, 44(6), 2782-2791.

Karla Salvagni, H., Matthew Richard, C., and Nilo Cesar, C. (2005). "Effect of Microreinforcement of Soils from Very Small to Large Shear Strains." *Journal of Geotechnical and Geoenvironmental Engineering*, 131(8), 1024-1033.

Liu, J., Wang, G., Kamai, T., Zhang, F., Yang, J., and Shi, B. (2011). "Static liquefaction behavior of saturated fiber-reinforced sand in undrained ring-shear tests." *Geotextiles and Geomembranes*, 29(5), 462-471.

Maher, M. H., and Gray, D. H. (1990). "Static Response of Sands Reinforced with Randomly Distributed Fibers." *Journal of Geotechnical Engineering*, 116(11), 1661-1677.

Miranda Pino, L. F., and Baudet, B. A. (2015). "The effect of the particle size distribution on the mechanics of fibre-reinforced sands under one-dimensional compression." *Geotextiles and Geomembranes*, 43(3), 250-258.

Muir Wood, D., and Maeda, K. (2007). "Changing grading of soil: effect on critical states." *Acta Geotech.*, 3(1), 3-14.

Nguyen, L., and Fatahi, B. (2016). "Behaviour of clay treated with cement & fibre while capturing cementation degradation and fibre failure – C3F Model." *International Journal of Plasticity*, 81, 168-195.

Oldecop, L. A., and Alonso, E. E. (2007). "Theoretical investigation of the time-dependent behaviour of rockfill." *Géotechnique*, 57(3), 289-301.

Salah, S., Shadi, S. N., and Fadi, F. (2010). "Shear Strength of Fiber-Reinforced Sands." *Journal of Geotechnical and Geoenvironmental Engineering*, 136(3), 490-499.

Santoni, R. L., Tingle, J. S., and Webster, S. L. (2001). "Engineering Properties of Sand-Fiber Mixtures for Road Construction." *Journal of Geotechnical and Geoenvironmental Engineering*, 127(3), 258-268.

Santos, A. P. S. D., Consoli, N. C., and Baudet, B. A. (2010). "The mechanics of fibre-reinforced sand." *Géotechnique*, 60(10), 791-799.

Tang, C.-S., Li, J., Wang, D.-Y., and Shi, B. (2016). "Investigation on the interfacial mechanical behavior of wave-shaped fiber reinforced soil by pullout test." *Geotextiles and Geomembranes*, 44(6), 872-883.

Wang, X. Z., Jiao, Y. Y., Wang, R., Hu, M. J., Meng, Q. S., and Tan, F. Y. (2011). "Engineering characteristics of the calcareous sand in Nansha Islands, South China Sea." *Engineering Geology*, 120(1-4), 40-47.

Wei, H., Zhao, T., He, J., Meng, Q., and Wang, X. (2018). "Evolution of Particle Breakage for Calcareous Sands during Ring Shear Tests." *International Journal of Geomechanics*, 18(2), 04017153.

Wu, Y., Yoshimoto, N., Hyodo, M., and Nakata, Y. (2014). "Evaluation of crushing stress at critical state of granulated coal ash in triaxial test." *Géotechnique Letters*, 4(4), 337-342.

Yetimoglu, T., and Salbas, O. (2003). "A study on shear strength of sands reinforced with randomly distributed discrete fibers." *Geotextiles and Geomembranes*, 21(2), 103-110.

Yu, F. W. (2017). "Particle Breakage and the Drained Shear Behavior of Sands." *International Journal of Geomechanics*, 17(8).

Yu, F. W. (2017). "Particle breakage and the critical state of sands." *Géotechnique*, 67(8), 713-719.

Zhang, S., Tong, C.-X., Li, X., and Sheng, D. (2015). "A new method for studying the evolution of particle breakage." *Géotechnique*, 65(11), 911-922.

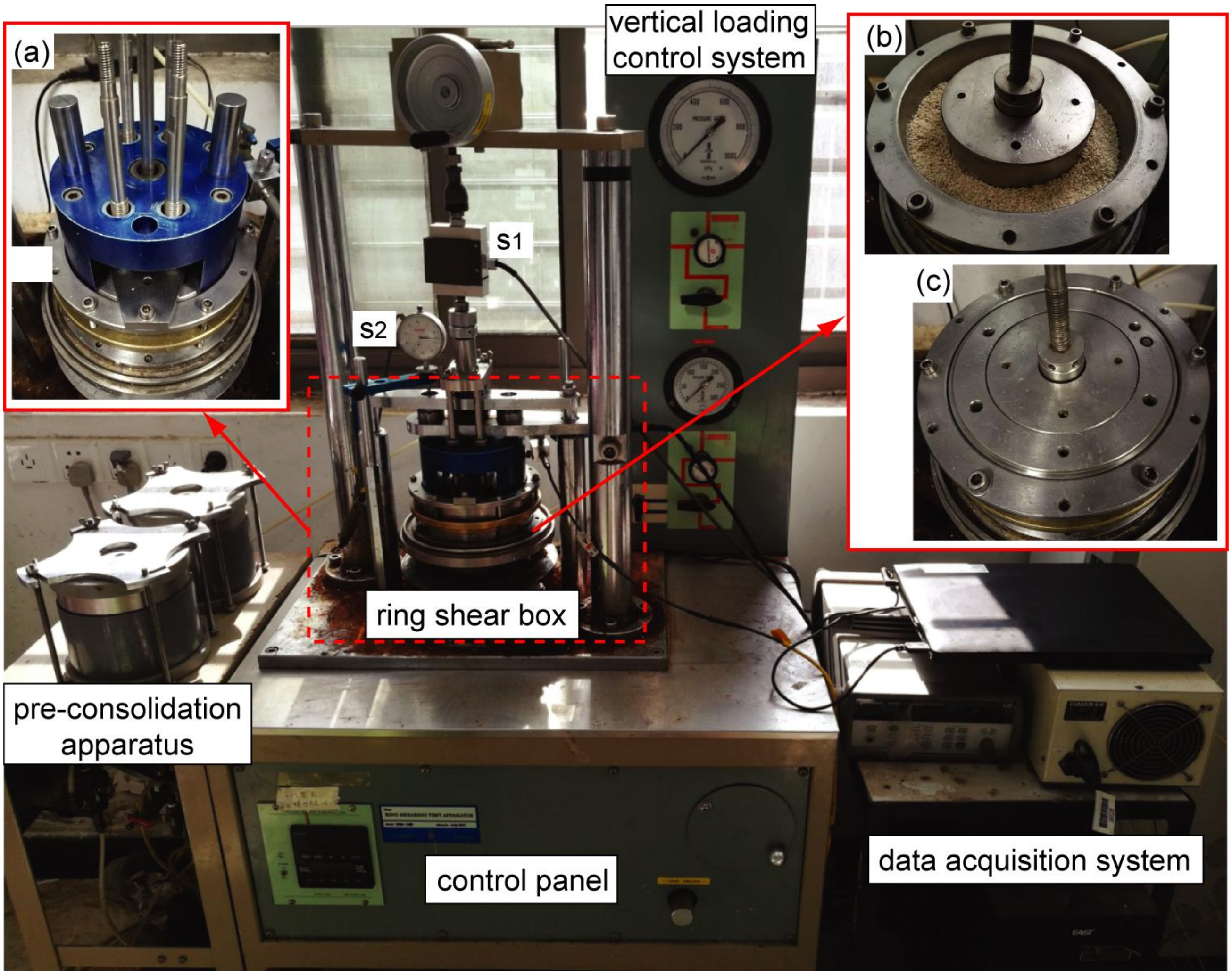

Fig. 1. The ring shear test apparatus. (a): shear box fixed on the testing rig; (b) shear box filled with calcareous sands; (c) shear box covered by porous stone disc and upper loading plate. ‘s1’: vertical loading load cell; ‘s2’: vertical displacement dial gauge transducer.

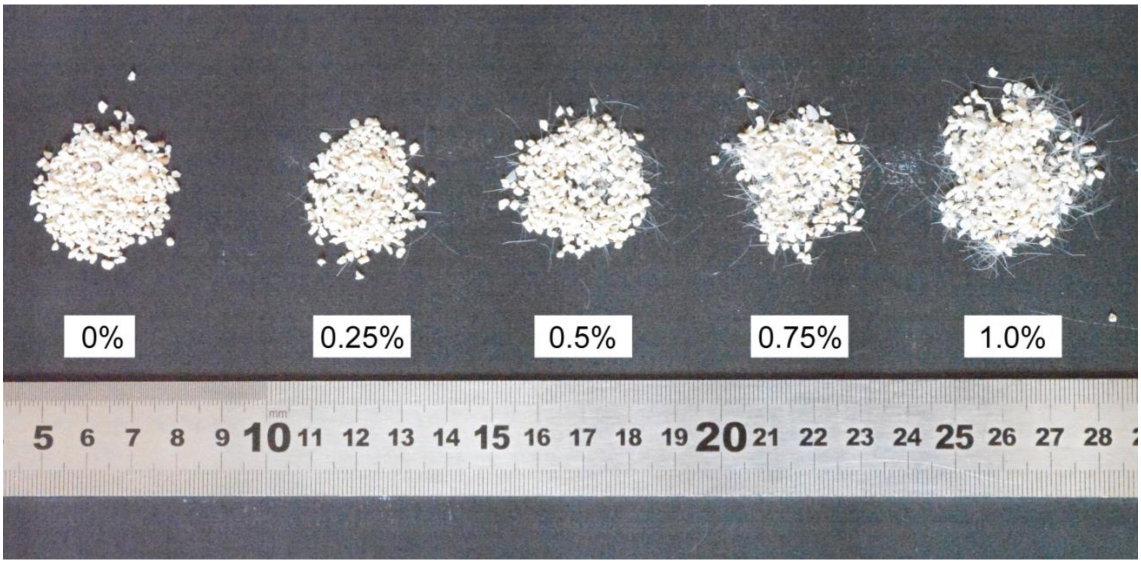

Fig. 2. Fibre-calcareous sand mixtures with different fibre contents.

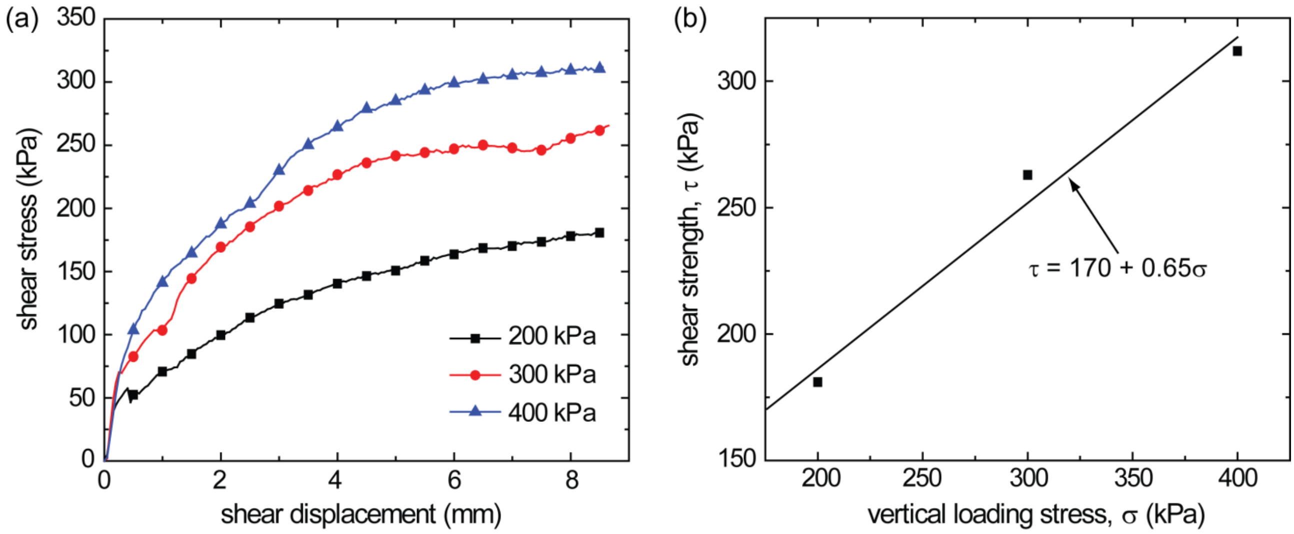

Fig. 3. Evolution of shear stress under different vertical loading stresses (ρ_f=0.5%, l=9 mm).

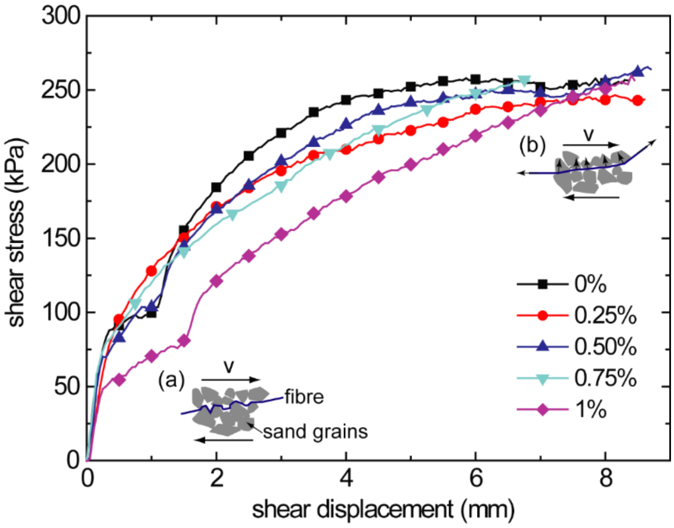

Fig. 4. Evolution of shear stress for tests with different fibre contents (σ = 300 kPa, l=9 mm).

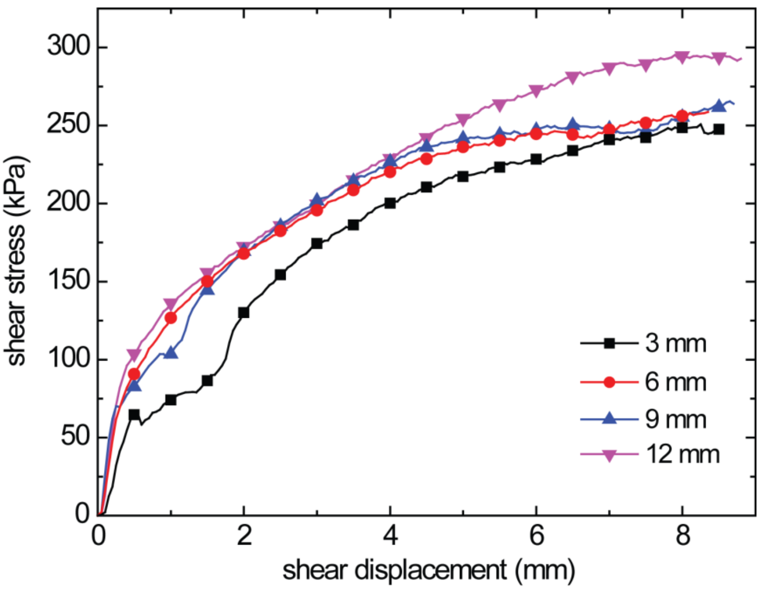

Fig. 5. Evolution of shear stress for tests with different fibre lengths (σ = 300 kPa, α=0.5%).

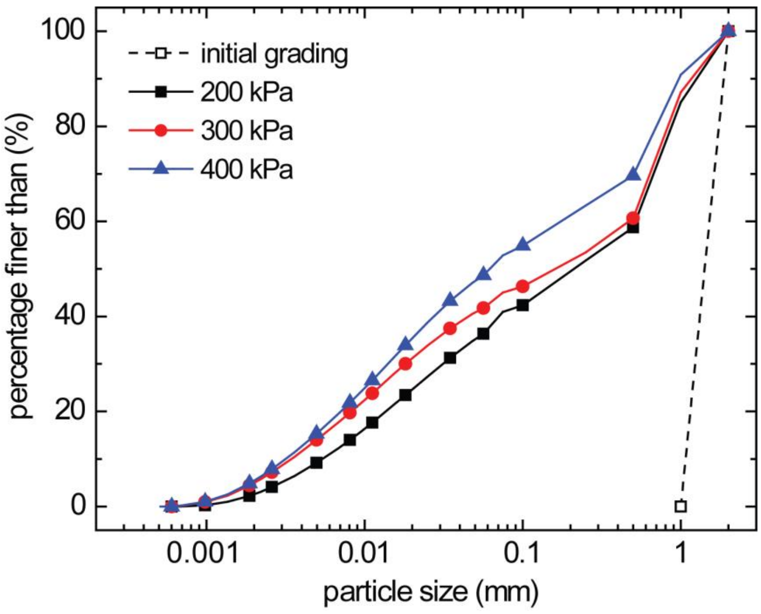

Fig. 6. PSD of the calcareous sands in the shear band for tests under different vertical loading stresses (α=0.5%, l=9 mm).

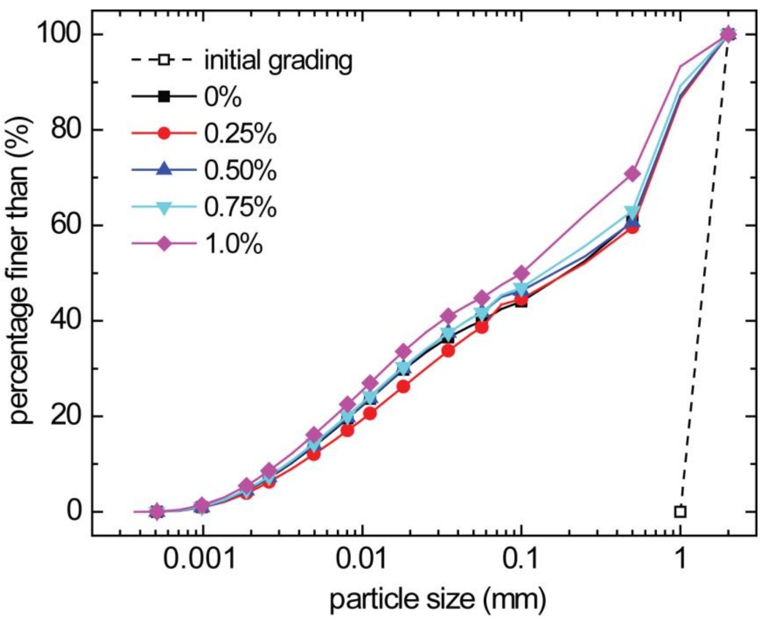

Fig. 7. PSD of the calcareous sands in the shear band for tests with different fibre contents (σ = 300 kPa, l=9 mm).

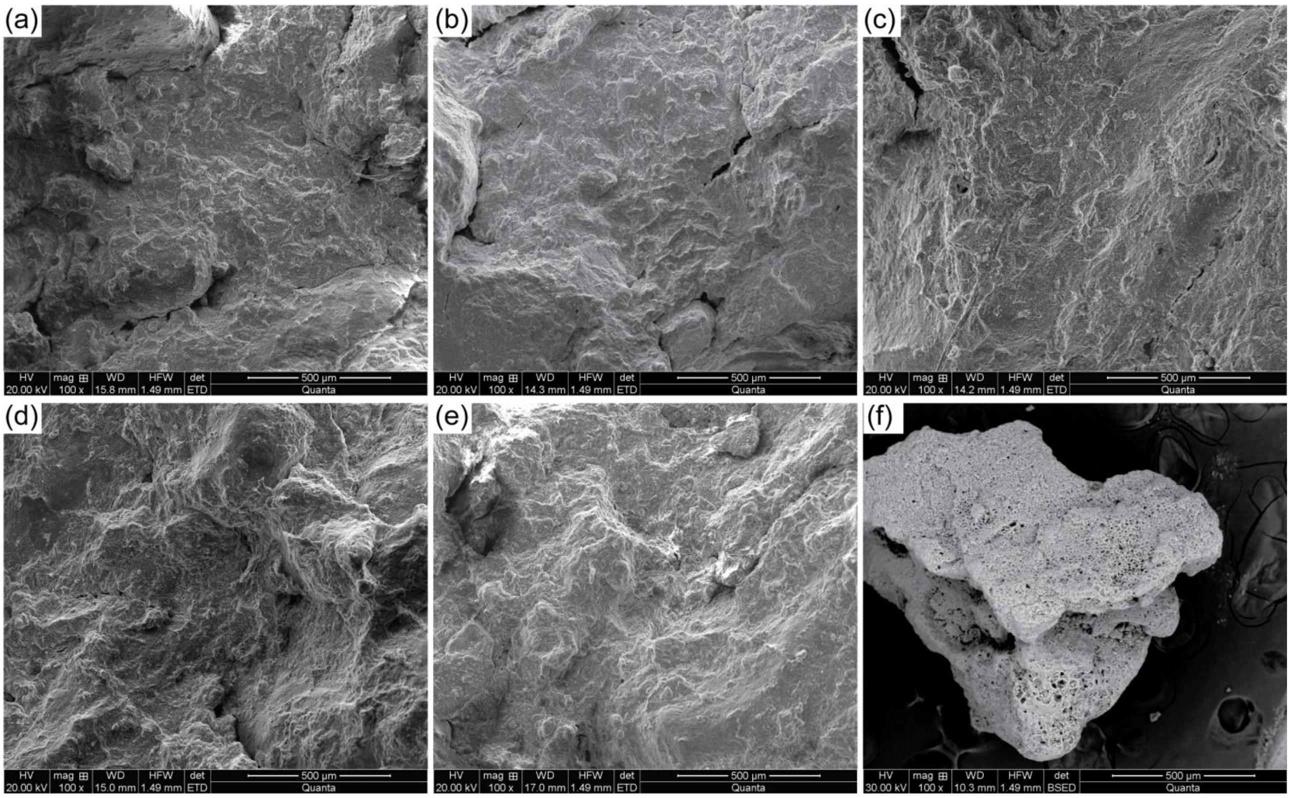

Fig. 8. SEM images of calcareous sand specimen after the RS tests. Figure (a)-(e) are the results of tests with fibre content of 0%, 0.25%, 0.5%, 0.75% and 1%, respectively. Figure (f) is the image of a single calcareous sand particle.

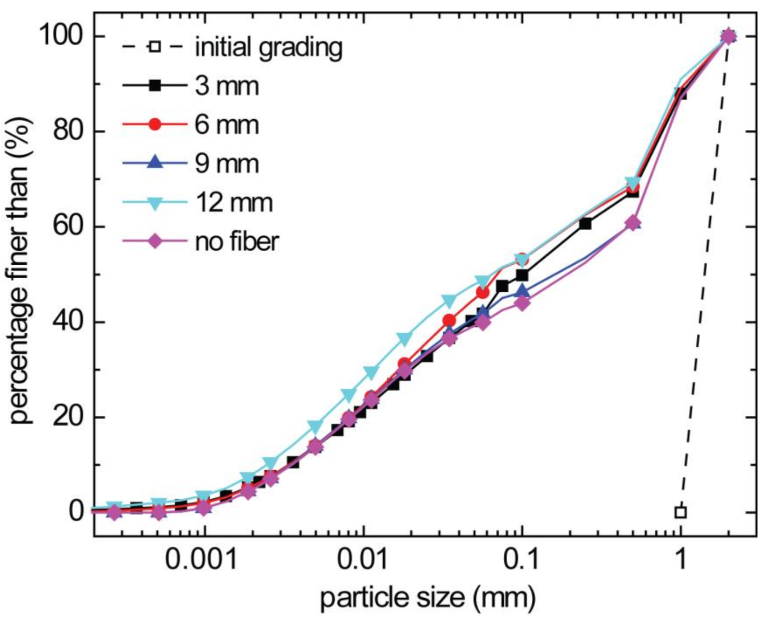

Fig. 9. PSD of the calcareous sands in the shear band for tests with different fibre lengths (σ = 300 kPa, α=0.5%).

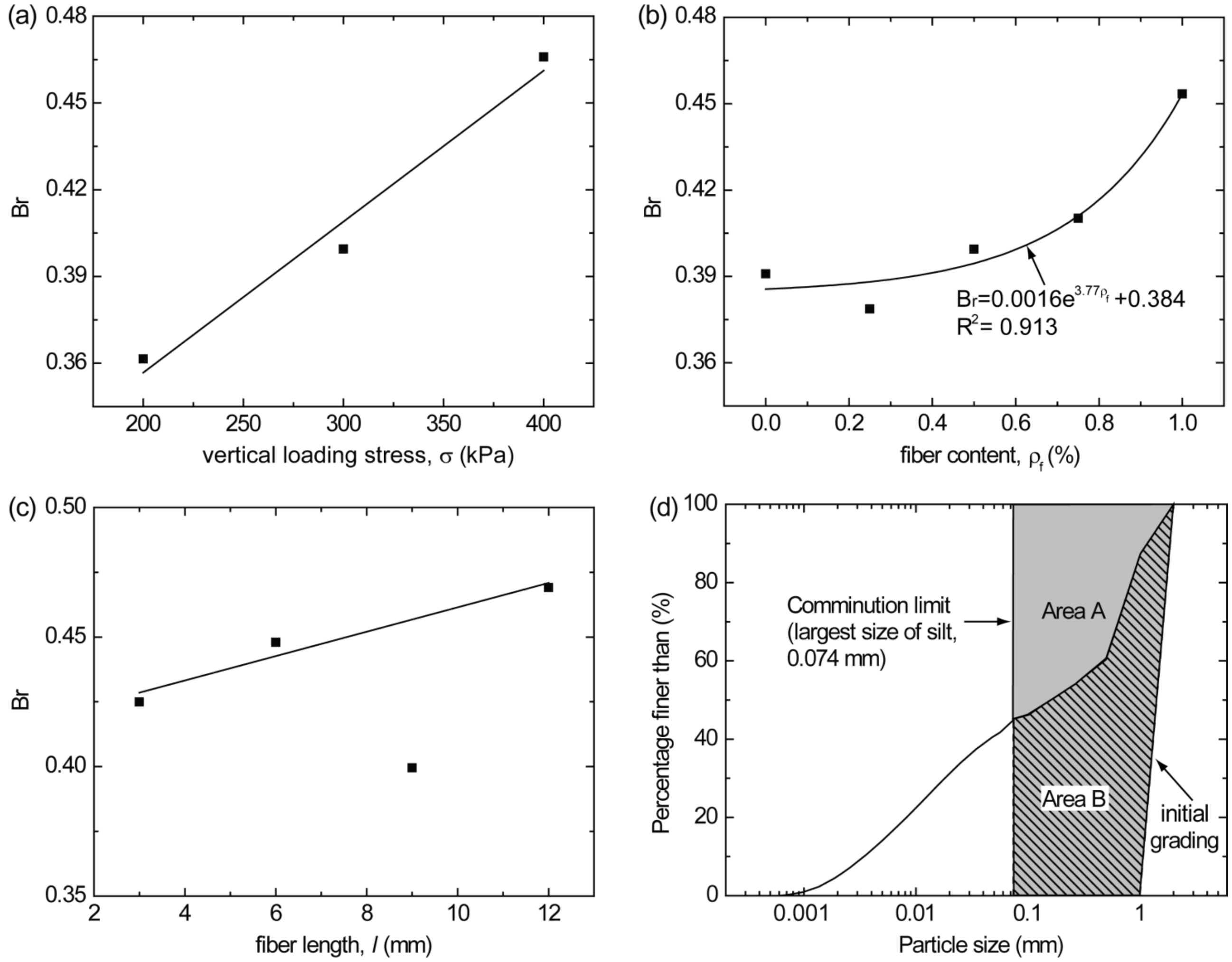

Fig. 10. Relative breakage of calcareous sands for tests (a) under different vertical loading stresses (α=0.5%, l=9 mm), (b) with various fibre contents (σ = 300 kPa, l=9 mm), and (c) with different fibre lengths ((σ = 300 kPa, α=0.5%)). The plot (d) illustrates the definition of relative breakage, B_r, as the ratio of total particle breakage (area B) to the potential breakage (area A+B).

Table 1. Properties of calcareous sands and polypropylene fibers. The properties of the polypropylene fibers are provided by the manufacturer (Zhengzhou Zhonghui Chemical Products Co. LTD, China).

Properties of calcareous sands

diameter (mm)	density (kg/m^3)	bulk density (kg/m^3)	void ratio
1-2	2790	1030-1170	1.38-1.71

Properties of polypropylene fibers

diameter (μm)	density (kg/m^3)	tensile strength (MPa)	modulus of elasticity (GPa)
31	910	400	3.5